

LETTER

A method for controlling alkali-metal oxide activities in one-atmosphere experiments and its application to measuring the relative activity coefficients of $\text{NaO}_{0.5}$ in silicate melts

HUGH ST. C. O'NEILL*

Research School of Earth Sciences, Australian National University, Canberra, ACT 0200, Australia

ABSTRACT

The activity of alkali metal oxides can be controlled in one-atmosphere wire-loop experiments at high temperature by suspending a crucible containing alkali silicate melt beneath the samples. The method has been applied to measuring the activity coefficient of $\text{NaO}_{0.5}$ in a series of CMAS- $\text{NaO}_{0.5}$ melts relative to that in the anorthite-diopside eutectic composition at 1400 °C, using a reservoir of $\text{NaO}_{0.5}$ - SiO_2 melt. The results show that this relative activity coefficient decreases strongly with SiO_2 , increases with CaO and MgO , but is insensitive to $\text{AlO}_{1.5}$. This latter behavior is inconsistent with “quasi-crystalline” models of melt thermodynamics that hypothesize Na-Al species.

INTRODUCTION

A well-known problem afflicting high-temperature experiments at atmospheric pressure or under vacuum is loss of alkalis by volatilization (e.g., Donaldson et al. 1975; Donaldson 1979; Corrigan and Gibb 1979; Appora et al. 2003). In extreme cases of high temperatures, low f_{O_2} , small sample sizes, and long run times, the alkali elements may be lost almost entirely from the experimental charge (e.g., O'Neill and Mavrogenes 2002). The wire-loop method of suspending samples is particularly vulnerable to alkali loss (Donaldson et al. 1975), but such loss is also observed in stirred-crucible experiments (Ertel et al. 1997). Yet it is often also observed that intended alkali-free compositions become contaminated in one-atmosphere experiments from alkalis lost from previous experiments in the same furnace. Furthermore, alkalis often seem to exchange between wire-loop samples run adjacent to each other; for example, Appora et al. (2003, p. 465) reported that “glasses with initially different Na contents approach a common major-element composition (in some cases including increases of Na-poor glasses loaded adjacent to Na-rich glasses) over the course of an experiment, suggesting that Na is not only lost but also exchanged between adjacent melt drops.” In fact, the Na exchange between samples in an experiment appears to be quite remarkably quantitative, as the example shown in Figure 1 from my own work demonstrates.

Here I discuss a method of controlling alkali metal oxide activities in one-atmosphere experiments based on these observations. I have recently used the method to investigate the effects of $\text{NaO}_{0.5}$ on the solubilities of S in silicate melts at low f_{O_2} , extending previous work reported in O'Neill and Mavrogenes (2002), and on the activity coefficients of Ni and Co in CMAS- $\text{NaO}_{0.5}$ melts, extending the previous work on CaO-MgO- $\text{AlO}_{1.5}$ - SiO_2 (CMAS) melts reported in O'Neill and Eggins (2002). These new results will be presented elsewhere; here, I showcase the method by reporting a preliminary investigation on how the activity coefficients of $\text{NaO}_{0.5}$ in silicate melts ($\gamma_{\text{NaO}_{0.5}}$) vary in the system CMAS at

1400 °C. Of particular interest is testing the hypothesis widely adopted in the geological literature that the thermodynamics of silicate melts can be modelled appropriately using components that reflect the stoichiometries of the crystals in equilibrium with the melts between their solidi and liquid (the “quasi-crystalline” model; Hess 1977; Burnham 1981; Ghiorso and Sack 1995; Holland and Powell 2001). Alkali metals occur in common rock-forming minerals coupled with Al (e.g., for Na, some common components are $\text{NaAlSi}_3\text{O}_8$ in nepheline, $\text{NaAlSi}_3\text{O}_8$ in feldspar, and $\text{NaAlSi}_2\text{O}_6$ in clinopyroxene), which, in the quasi-crystalline hypothesis, implies Na-Al interactions in the melts. Thermodynamically, the formation of a complex between components in a silicate melt causes negative departures from ideal mixing (e.g., Navrotsky 1995; Hess 1995), hence the hypothetical Na-Al interactions should result in a decrease in the activity coefficient of $\text{NaO}_{0.5}$ as the $\text{AlO}_{1.5}$ content in the melt increases, if the relative mole fractions of other components are held constant. This is readily tested with the method described here.

EXPERIMENTAL STRATEGY

The method has the virtue of being very simple and easy to implement. Typically, samples in one-atmosphere gas-mixing experiments are attached to wire loops (e.g., Donaldson et al. 1975); in my laboratory, the loops are then suspended, several at a time, from a “chandelier” made of thick Pt wire, as described in O'Neill and Mavrogenes (2002) and O'Neill and Eggins (2002). The control of $\text{NaO}_{0.5}$ activity is achieved by hanging an open Pt crucible containing a suitable composition on the join $\text{NaO}_{0.5}$ - SiO_2 a few centimeters beneath the “chandelier.” Obviously any alkali oxide-silica mixture can be used as required ($\text{KO}_{0.5}$ - SiO_2 , $\text{NaO}_{0.5}$ - $\text{KO}_{0.5}$ - SiO_2 , etc.). The crucible contains 5 to 10 g of melt, thus providing a reservoir of the alkali oxide that is 10^2 to 10^3 times that in the samples (which typically weigh <100 mg each). Alkali evaporates from the surface of the crucible [$\text{NaO}_{0.5}$ (reservoir) \rightarrow $\text{Na(g)} + 1/4 \text{ O}_2$], bathing the samples in alkali vapor, which dissolves in the samples [$\text{Na(g)} + 1/4 \text{ O}_2 \rightarrow \text{NaO}_{0.5}$ (sample)]. As implied by the data in Figure 1, the alkali loss out of the hot zone of the furnace is slow, and a time series

* E-mail: hugh.oneill@anu.edu.au

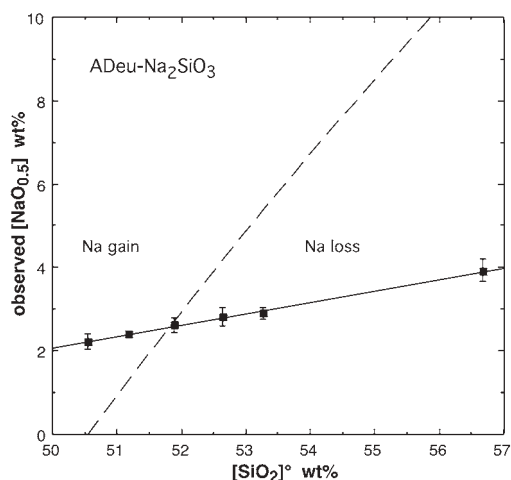


FIGURE 1. Sodium exchange among compositions from a conventional wire-loop experiment (B26/3/02) on the join ADeu–Na₂SiO₃, run at 1400 °C, $f_{O_2} = 10^{-12}$ bars, 118 hours. Compositions are the means of six analyses, error bars are $\pm 2\sigma$, and SiO₂ is plotted renormalized to an Na-free basis ([SiO₂][°]). The intended compositions would fall on the dashed curve. Final compositions show both Na gain (the two samples lowest in SiO₂) and Na loss. The remarkably regular correlation between final [NaO_{0.5}] and [SiO₂][°] is explained by assuming constant $a_{NaO_{0.5}}^{sample}$ among the samples, with the correlation caused by decreasing $\gamma_{NaO_{0.5}}$ with increasing SiO₂.

of three replicate experiments (in air) shows that a steady state is reached within 8.5 hours, and is maintained for several days at least. Because f_{O_2} cancels out between the evaporation and condensation of Na(g), it might have been presumed that the steady state corresponds to equilibrium between reservoir and samples (i.e., $a_{NaO_{0.5}}^{sample} = a_{NaO_{0.5}}^{reservoir}$), but this is found not to be the case. Instead, it is observed that the concentration of NaO_{0.5} in a sample increases with decreasing f_{O_2} at constant NaO_{0.5}/SiO₂ in the reservoir, indicating that the steady state is controlled partly by the rate of evaporation, which increases with decreasing f_{O_2} , because the dominant Na species in the gas phase is monatomic Na. Also, keeping all other factors constant, the amount of NaO_{0.5} in a sample is found to depend on how far the reservoir is hung below the samples. Positioning the reservoir ~10 cm below the samples allows the latter to be bathed more evenly in the Na vapor than if the reservoir is nearer, giving greater reproducibility as judged from replicate runs; but the reservoir is then displaced from the hot-spot of the furnace, precluding true equilibrium with the samples (for 10 cm below, ΔT is about 30 °C at 1400 °C in the furnace used for this study).

My strategy, therefore, has been to accept that the activities of NaO_{0.5} in the samples will not be the same as in the reservoir, but rather to make use of the observation, based on replicate measurements (see below) that $a_{NaO_{0.5}}^{sample}$ is the same for all samples in a set in any given experiment, when the reservoir is hung sufficiently far below the samples. By definition:

$$a_{NaO_{0.5}} = X_{NaO_{0.5}} \gamma_{NaO_{0.5}} \quad (1)$$

Let one of the compositions in the experiment be a standard reference composition, used in all experiments. The hypothesis of constant $a_{NaO_{0.5}}^{sample}$ then gives:

$$\gamma_{NaO_{0.5}}^{sample} = (X_{NaO_{0.5}}^{ref} / X_{NaO_{0.5}}^{sample}) \gamma_{NaO_{0.5}}^{ref} \quad (2)$$

The anorthite-diopside eutectic composition (hereafter ADeu) was chosen as the reference melt, although any relatively low-melting composition that does not include volatiles or heterovalent elements like Fe would be suitable. Normalizing to a standard reference composition included among the samples avoids the difficulties of retrieving and accurately analyzing the NaO_{0.5}–SiO₂ melts in the reservoir. Nevertheless, it is obviously useful to establish an empirical understanding of the variation between the NaO_{0.5}/SiO₂ ratio in the reservoir and NaO_{0.5} in the samples as a function of experimental variables such as f_{O_2} , temperature, and reservoir position, so that the reservoir composition can be set to achieve a desired concentration of NaO_{0.5} as closely as possible. In practice, experience with a few runs at a given temperature and f_{O_2} is all that is required to anticipate the resulting NaO_{0.5} content of the ADeu standard melt to ± 1 wt%. The method works down to 1200 °C at least; presumably it could be implemented at lower temperature using, for example, NaO_{0.5}–WO₃ melts.

Two experimental drawbacks need to be mentioned. First, once an alumina muffle tube has been used for an experiment with an alkali silicate reservoir it becomes contaminated with the alkali element in question, potentially contaminating the samples in subsequent experiments. Secondly, because alkalis can be anticipated to poison thermocouples, the temperature was measured external to the muffle tube (relying on the thermocouple used for temperature control) rather than directly over the samples. For the same reason, no attempt was made to monitor f_{O_2} with an oxygen sensor (although this is not relevant to the experiments reported here).

The method as outlined above may be viewed as a development of previous ideas on imposing an alkali metal vapor pressure in one-atmosphere experiments. Lewis et al. (1993) evaporated NaCl in a muffle furnace to provide a Na vapor to react with melts of chondrule-like composition. Georges et al. (2000) used a mixture of K₂CO₃ with graphite to produce a K vapor, also to study chondrule formation.

EXPERIMENTAL DETAILS

Sodium-free silicate melt compositions were prepared from oxides and carbonates, and mounted as beads on wire loops as described previously (O'Neill and Mavrogenes 2002; O'Neill and Eggins 2002). The NaO_{0.5}–SiO₂ reservoir mixtures were made from Na₂SiO₃·5H₂O and SiO₂·*n*H₂O, both dehydrated at 900 °C before weighing. The mixture was loaded into the Pt crucible used for the reservoir and further dehydrated in a box furnace by heating slowly to 1100 °C, which is just above the melting point of Na₂SiO₃. The reservoir crucible was then suspended from the middle of the “chandelier” holding 6 to 8 samples, and the assembly introduced into a vertical tube furnace equipped for gas-mixing at 600 °C. The temperature was then increased at 6 °C/min to the final run temperature of 1400 °C (the experimental temperature of all results reported here).

The majority of the experiments reported here were done in air; usually this was made to flow through the furnace at a low rate (~50 cm³/min) using an aquarium pump, but several runs were also made without a controlled air flow, both with the furnace closed, making for a static atmosphere, and with the bottom left open. These variations appear to have had no discernible effect. The technique has also been used exactly as described here with CO–CO₂, CO–CO₂–SO₂, and O₂–SO₂ gas mixtures. Samples were drop-quenched into water, the reservoir dropping at the same time. The reservoir can be recovered, dried, and used again if a similar $a_{NaO_{0.5}}$ is required for the next experiment. The quenched glass samples were mounted in epoxy and polished for electron microprobe analysis, which was carried out using the CAMECA Camebax at the RSES, ANU, in the EDS mode. Standardization and ZAF correction procedures are described in Ware (1981). Operating conditions

were 15 kV and 6 nA, a counting time of 100 live seconds, and beam defocused to $\sim 10 \mu\text{m}$ to minimize Na loss. A series of analyses using a beam rastered over 25, 50, and $100 \mu\text{m}$ squares indicated that the amount of Na loss is negligible for the glass compositions reported here (Na loss under the electron beam is a problem more in hydrous glasses). Glasses were in all cases found to be very homogenous; the observed precision to which $[\text{NaO}_{0.5}]$ is determined is generally $\sim 2\%$ (1σ) for $[\text{NaO}_{0.5}] > 2 \text{ wt\%}$.

RESULTS

Figure 2 shows the results for 11 runs on a set of six compositions (called AD6) in the system CMAS $\pm \text{TiO}_2$, which have been used in the recent studies of O'Neill and Mavrogenes (2002) and O'Neill and Eggins (2002); the analysed Na-free compositions are tabulated in both references. These runs were made at different f_{O_2} values and reservoir $\text{NaO}_{0.5}/\text{SiO}_2$ ratios, which produces a series of compositions on binary joins of the type ADeu- $\text{NaO}_{0.5}$, etc. The results are plotted as the mole fraction $X_{\text{NaO}_{0.5}}$ against that in the ADeu "reference" sample ($X_{\text{NaO}_{0.5}}^{\text{ADeu}}$) in the same run.

In each individual experiment, $X_{\text{NaO}_{0.5}}$ decreases in the sequence $\text{AD} + \text{Qz} \gg \text{AD} + \text{TiO}_2 > \text{AD} + \text{En} > \text{ADeu} > \text{AD} + \text{Fo} \gg \text{AD} + \text{Wo}$, implying the reverse sequence of activity coefficients. Note that varying f_{O_2} at constant reservoir $\text{NaO}_{0.5}/\text{SiO}_2$ causes fairly substantial changes in the values of $X_{\text{NaO}_{0.5}}$ recorded in the samples (the lower the f_{O_2} , the higher the $X_{\text{NaO}_{0.5}}$), but, nevertheless, runs at different f_{O_2} plot on the same curves; this result would be difficult to explain if the values of $X_{\text{NaO}_{0.5}}$ relative to each other depended on non-equilibrium effects. The data for $\text{AD} + \text{TiO}_2$, $\text{AD} + \text{En}$, and $\text{AD} + \text{Fo}$, for which the values of $X_{\text{NaO}_{0.5}}$ are close to those for ADeu, plot as straight lines, more or less, but the data for $\text{AD} + \text{Qz}$ and $\text{AD} + \text{Wo}$ show distinct curvature (parabolic), with both curves trending toward the 1:1 line on the plot as $X_{\text{NaO}_{0.5}}$ increases. This behavior is expected, as for all compositions $\gamma_{\text{NaO}_{0.5}} \rightarrow 1$ as $X_{\text{NaO}_{0.5}} \rightarrow 1$ by definition,

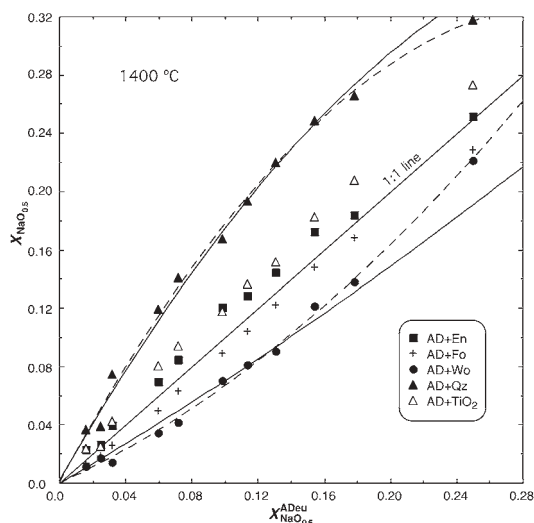


FIGURE 2. Solubility of $\text{NaO}_{0.5}$ in AD6 compositions relative to that in the ADeu "reference" composition. The experiment with the highest $\text{NaO}_{0.5}$ was produced with pure Na_2SiO_3 in the reservoir at $f_{\text{O}_2} = 10^{-6.7}$ bars; most other runs were done in air. Solid curves are best fits for $\text{AD} + \text{Qz}$ and $\text{AD} + \text{Wo}$ compositions to Equation 5, omitting the highest Na datum. The dashed curves are from Equation 6, and include the highest Na datum.

hence the differences among values of $\gamma_{\text{NaO}_{0.5}}$ must diminish as $X_{\text{NaO}_{0.5}}$ increases.

To quantify the relations shown in Figure 2, consider the following simplified theory. For the regular solution formalism, which is the simplest way to represent deviations from ideality in a solution as a function of composition, it can be shown that:

$$\ln \gamma_{\text{NaO}_{0.5}} = (1 - X_{\text{NaO}_{0.5}})^2 \ln \gamma_{\text{NaO}_{0.5}}^{\infty} \quad (3)$$

where $\gamma_{\text{NaO}_{0.5}}^{\infty}$ is the Henry's law activity coefficient in the melt as $X_{\text{NaO}_{0.5}} \rightarrow 0$. Darken (1967a, 1967b) famously argued that this relationship holds well even for systems that are not strictly regular over their entire compositional range (Darken's "quadratic formalism"), and this equation has been used by Nicholls (1980) to model the solubility of H_2O in silicate melts. Invoking the hypothesis of equal $a_{\text{NaO}_{0.5}}$ in all samples in one experiment and selecting the ADeu composition as the reference composition then gives:

$$\ln X_{\text{NaO}_{0.5}} = \ln X_{\text{NaO}_{0.5}}^{\text{ADeu}} + (1 - X_{\text{NaO}_{0.5}}^{\text{ADeu}})^2 \ln \gamma_{\text{NaO}_{0.5}}^{\text{ADeu},\infty} - (1 - X_{\text{NaO}_{0.5}})^2 \ln \gamma_{\text{NaO}_{0.5}}^{\infty} \quad (4)$$

Unfortunately, the value of $\gamma_{\text{NaO}_{0.5}}^{\text{ADeu},\infty}$ is not known a priori and it cannot be derived in the present study because the term $(1 - X_{\text{NaO}_{0.5}}^{\text{ADeu}})^2 \ln \gamma_{\text{NaO}_{0.5}}^{\text{ADeu},\infty}$ is highly correlated with $(1 - X_{\text{NaO}_{0.5}})^2 \ln \gamma_{\text{NaO}_{0.5}}^{\infty}$ for all compositions. As a provisional expedient, therefore, I have used the approximation:

$$\ln X_{\text{NaO}_{0.5}} \cong \ln X_{\text{NaO}_{0.5}}^{\text{ADeu}} - (1 - X_{\text{NaO}_{0.5}})^2 \ln(\gamma_{\text{NaO}_{0.5}}^{\infty} / \gamma_{\text{NaO}_{0.5}}^{\text{ADeu},\infty}) \quad (5)$$

noting that this relationship becomes increasingly valid as $X_{\text{NaO}_{0.5}} \rightarrow 0$ or as $\gamma_{\text{NaO}_{0.5}}^{\text{ADeu},\infty}$ becomes similar to $\gamma_{\text{NaO}_{0.5}}^{\infty}$. This equation would also be valid if $\gamma_{\text{NaO}_{0.5}}^{\text{ADeu},\infty} = 1$ (ideal solution of $\text{NaO}_{0.5}$ in ADeu melt), but this seems unlikely. In fact, Equation 5 fits the data well, as shown in Figure 3, except for the $\text{AD} + \text{Qz}$ and $\text{AD} + \text{Wo}$ compositions in the experiment with the highest $[\text{NaO}_{0.5}]$. It is remarkable, nevertheless, that an empirical fit to a simple second-order polynomial:

$$X_{\text{NaO}_{0.5}} = a_1 X_{\text{NaO}_{0.5}}^{\text{ADeu}} + a_2 (X_{\text{NaO}_{0.5}}^{\text{ADeu}})^2 \quad (6)$$

can reproduce all data (Fig. 3); the smoothness of these fits implies an experimental uncertainty $\sigma([\text{NaO}_{0.5}]) = 0.02 [\text{NaO}_{0.5}] + 0.1 \text{ wt\%}$, close to the observed precision of the analytical data alone.

The empirical nature of Equation 6 makes it unsuitable for extracting relative activity coefficients, not least because of the correlation between a_1 and a_2 , whereas the single parameter in Equation 5 is determined robustly, leading to unambiguous values of $\gamma_{\text{NaO}_{0.5}}^{\infty} / \gamma_{\text{NaO}_{0.5}}^{\text{ADeu},\infty}$ as $X_{\text{NaO}_{0.5}} \rightarrow 0$.

It is perhaps surprising that such a simple relationship can fit the data over such a large range of $X_{\text{NaO}_{0.5}}$; the higher values of $X_{\text{NaO}_{0.5}}$ shown in Figure 2 exceed considerably those found in natural silicate magmas. They also cross the divide between peraluminous and peralkaline compositions (this occurs at $X_{\text{NaO}_{0.5}} = 0.14, 0.07$, and 0.10 for the ADeu, $\text{AD} + \text{Wo}$, and $\text{AD} + \text{Qz}$ compositions, respectively), with no change in behavior apparent. Because it is possible that any such change in $\gamma_{\text{NaO}_{0.5}}$ at the peralkaline/peraluminous transition in this series of experi-

ments could be obscured if it cancelled out between the ADeu “reference” and the other samples, I have carried out a series of experiments on five compositions in the join $\text{CaMgSi}_2\text{O}_6\text{--AlO}_{1.5}$ (Di-Cor). The results are summarized in Figure 3, from where it may be confirmed that there is no inflection in $\gamma_{\text{NaO}_{0.5}}$ at the peralkaline/peraluminous transition. This is a significant result

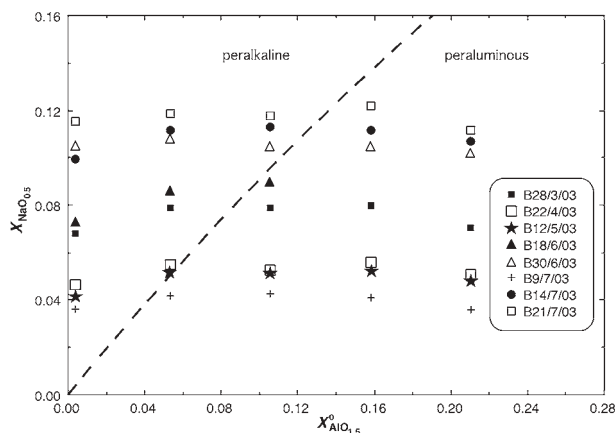


FIGURE 3. The effect of $\text{AlO}_{1.5}$ on the solubility of $\text{NaO}_{0.5}$ in compositions on the join Di-Cor. The transition from melts with molar $\text{Na}/\text{Al} < 1$ (peraluminous) to $\text{Na}/\text{Al} > 1$ (peralkaline) is indicated by the dashed curve. There appears to be no effect on the solubility of $\text{NaO}_{0.5}$ on crossing this compositional threshold. Two compositions from B18/6/03 were lost.

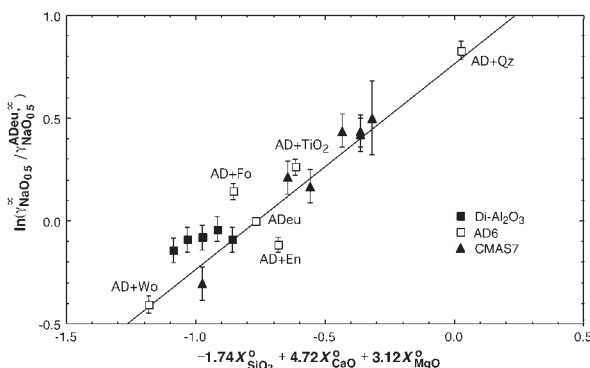


FIGURE 4. Effects of SiO_2 , CaO , and MgO on $\gamma_{\text{NaO}_{0.5}}^{\text{ADeu},\infty} / \gamma_{\text{NaO}_{0.5}}^{\text{ADeu},0}$ (see text for details). Error bars $\pm 2\sigma$.

given the importance traditionally attached to this transition in several contexts in silicate melt studies, including the quasi-crystalline thermodynamic models that feature coupled Na-Al components. The lack of Na-Al interactions observed here is contrary to their apparent role in the partitioning of Na between clinopyroxene and silicate melt deduced by Blundy et al. (1995); see also the discussion of the “peralkaline effect” on the solubility of high valency cations by Hess (1995, pp. 166–172). On the other hand, the model of Ghiorso and Sack (1995) uses Na_2SiO_3 and not an Na-Al species as the component for $\text{NaO}_{0.5}$, but KAl-SiO_4 for $\text{KO}_{0.5}$. Whether this difference in approach derives from a real difference in the behavior of Na and K in silicate melts should be readily testable with the present method.

Values of $\gamma_{\text{NaO}_{0.5}}^{\infty} / \gamma_{\text{NaO}_{0.5}}^{\text{ADeu},\infty}$ decrease markedly with SiO_2 , as seen in AD + Qz, confirming the implication of the trend in Figure 1. This is not unexpected given the extraordinarily large interactions between $\text{NaO}_{0.5}$ and SiO_2 in melts in the system $\text{NaO}_{0.5}\text{--SiO}_2$ (Zaitsev et al. 1999); but $\gamma_{\text{NaO}_{0.5}}^{\infty} / \gamma_{\text{NaO}_{0.5}}^{\text{ADeu},\infty}$ increases with CaO (e.g., AD + Wo), which is perhaps less intuitive. Values of $\gamma_{\text{NaO}_{0.5}}^{\infty} / \gamma_{\text{NaO}_{0.5}}^{\text{ADeu},\infty}$ obtained from the AD6 series of experiments, the join Di-Cor, and from seven other CMAS compositions (CMAS7, see O'Neill and Mavrogenes 2002; O'Neill and Eggins 2002), are given in Table 1. To test for compositional correlations, these data were regressed against composition, giving:

$$\ln(\gamma_{\text{NaO}_{0.5}}^{\infty} / \gamma_{\text{NaO}_{0.5}}^{\text{ADeu},\infty}) = -0.77 - 1.74X_{\text{SiO}_2}^0 + 4.72X_{\text{CaO}}^0 + 3.12X_{\text{MgO}}^0 \quad (7)$$

where the X_i^0 , etc., are the mole fractions in the Na-free starting composition [i.e., $X_i^0 = X_i / (1 - X_{\text{NaO}_{0.5}}^0)$]. This correlation suggests that MgO has an influence similar to, but somewhat less than, CaO . As emphasized in Figure 4, this simple approach, although useful in revealing the influences on the thermodynamic behavior of $\text{NaO}_{0.5}$ in silicate melts, does not provide a quantitative description of $\gamma_{\text{NaO}_{0.5}}^{\infty} / \gamma_{\text{NaO}_{0.5}}^{\text{ADeu},\infty}$. In particular, the relative activity coefficients for AD + En and AD + Fo, which are very well determined (Fig. 2), are not well accounted for. Clearly, results on more compositions are required to understand these influences better, as would be direct measurements utilizing another technique on the activities of $\text{NaO}_{0.5}$ on the ADeu- $\text{NaO}_{0.5}$ binary join.

ACKNOWLEDGMENTS

Thanks to D. Dingwell and an anonymous reviewer for their reviews and to Bob Dymek for his expeditious editorial handling.

TABLE 1. Activity coefficients of $\text{NaO}_{0.5}$ in silicate melts at 1400 °C relative to that in the anorthite-diopside eutectic composition (ADeu), all at infinite dilution (see Eq. 5 in the text)

AD6* (11 runs)	$\ln \left(\frac{\gamma_{\text{NaO}_{0.5}}^{\infty}}{\gamma_{\text{NaO}_{0.5}}^{\text{ADeu},\infty}} \right)$	χ_v^{\dagger}	CMAS7* (5 runs)	$\ln \left(\frac{\gamma_{\text{NaO}_{0.5}}^{\infty}}{\gamma_{\text{NaO}_{0.5}}^{\text{ADeu},\infty}} \right)$	χ_v^{\dagger}	Di-Co (8 runs)	$\ln \left(\frac{\gamma_{\text{NaO}_{0.5}}^{\infty}}{\gamma_{\text{NaO}_{0.5}}^{\text{ADeu},\infty}} \right)$	χ_v^{\dagger}
AD+En	-0.144(19)	2.0	A	-0.44(4)	2.9	Di	0.14(3)	3.0
AD+Wo	0.155(18)	0.7	B†	-0.50(9)	1.9	Di ₉₅ Co ₅ §	0.09(3)	2.7
AD+Qz	0.405(21)	2.5	C	-0.21(4)	0.6	Di ₉₀ Co ₁₀ §	0.08(3)	4.2
AD+TiO ₂	-0.830(21)	1.8	D	-0.17(4)	1.3	Di ₈₅ Co ₁₅ §	0.04(3)	3.9
			E	0.30(4)	1.7	Di ₈₀ Co ₂₀ §	0.09(3)	1.1
			F	-0.44(4)	1.7			
			G	-0.42(4)	0.8			

* Compositions given in O'Neill and Mavrogenes (2002) and O'Neill and Eggins (2002).

† Reduced chi-squared, obtained from the fit assuming $\sigma[\text{Na}_2\text{O}] = 0.02[\text{Na}_2\text{O}] + 0.1 \text{ wt\%}$.

‡ The data for this composition have much higher scatter; the weighting of the data was increased to $\sigma[\text{Na}_2\text{O}] = 0.05[\text{Na}_2\text{O}] + 0.1 \text{ wt\%}$.

§ Compositions in wt%; i.e., Di₉₅Co₅ is 95 wt% $\text{CaMgSi}_2\text{O}_6$ and 5 wt% $\text{AlO}_{1.5}$.

REFERENCES CITED

- Appora, I., Eiler, J.M., Matthews, A., and Stolper, E.M. (2003) Experimental determination of oxygen isotope fractionations between CO₂ vapor and sodamelilite melt. *Geochimica et Cosmochimica Acta*, 67, 459–471.
- Blundy, J.D., Falloon, T.J., Wood, B.J., and Dalton, J.A. (1995) Sodium partitioning between clinopyroxene and silicate melts. *Journal of Geophysical Research*, 100B, 15501–15515.
- Burnham, C.W. (1981) The nature of multicomponent aluminosilicate melts. *Physics and Chemistry of the Earth*, 13, 197–226.
- Corrigan, G. and Gibb, F.G.F. (1979) Loss of Fe and Na from a basaltic melt during experiments using the wire-loop method. *Mineralogical Magazine*, 43, 121–126.
- Darken, L.S. (1967a) Thermodynamics of binary metallic solutions. *Transactions of the Metallurgical Society of AIME*, 239, 80–89.
- (1967b) Thermodynamics of ternary metallic solutions. *Transactions of the Metallurgical Society of AIME*, 239, 90–96.
- Donaldson, C.H. (1979) Composition changes in a basalt melt contained in a wire loop of Pt₈₀Rh₂₀; effects of temperature, time, and oxygen fugacity. *Mineralogical Magazine*, 43, 115–119.
- Donaldson, C.H., Williams, R.J., and Lofgren, G. (1975) Sample holding technique for study of crystal-growth in silicate melts. *American Mineralogist*, 60, 324–326.
- Ertel, W., Dingwell, D.B., and O'Neill, H. St.C. (1997) Compositional dependence of the activity of Ni in silicate melts. *Geochimica Cosmochimica Acta*, 61, 4707–4722.
- Georges, P., Libourel, G., and Deloule, E. (2000) Experimental constraints on alkali condensation in chondrule formation. *Meteoritics and Planetary Science* 35, 1183–1188.
- Ghiorso, M.S. and Sack, R.O. (1995) Chemical mass transfer in magmatic processes IV. A revised and internally consistent thermodynamic model for the interpolation and extrapolation of liquid-solid equilibria in magmatic systems at elevated temperatures and pressures. *Contributions to Mineralogy and Petrology*, 119, 197–212.
- Hess, P.C. (1977) Structure of silicate melts. *Canadian Mineralogist*, 15, 162–178.
- (1995) Thermodynamic mixing properties and the structure of silicate melts. In J. Stebbins, P.F. McMillan, and D.B. Dingwell, Eds., *Structure, Dynamics and Properties of Silicate Melts*, 32, 145–189. *Reviews in Mineralogy*, Mineralogical Society of America, Washington, D.C.
- Navrotsky, A. (1995) Energetics of silicate melts. In J. Stebbins, P.F. McMillan, and D.B. Dingwell, Eds., *Structure, Dynamics and Properties of Silicate Melts*, 32, 121–143. *Reviews in Mineralogy*, Mineralogical Society of America, Washington, D.C.
- Holland, T. and Powell, R. (2001) Calculation of phase relations involving haplogranitic melts using an internally consistent thermodynamic dataset. *Journal of Petrology*, 42, 673–683.
- Lewis, R.D., Lofgren, G., Franzen, H., and Windom, K.E. (1993) The effect of Na vapor on the Na content of chondrules. *Meteoritics*, 28, 622–628.
- Nicholls, J. (1980) A simple thermodynamic model for estimating the solubility of H₂O in magmas. *Contributions to Mineralogy and Petrology*, 74, 211–220.
- O'Neill, H.St.C. and Eggins, S.M. (2002) The effect of melt composition on trace element partitioning: an experimental investigation of the activity coefficients of FeO, NiO, CoO, MoO₂ and MoO₃ in silicate melts. *Chemical Geology*, 186, 151–181.
- O'Neill, H.St.C. and Mavrogenes, J.A. (2002) The sulfide capacity and the sulfur content at sulfide saturation of silicate melts at 1400°C and 1 bar. *Journal of Petrology*, 43, 1049–108.
- Ware, N.G. (1981) Computer programs and calibration with the PIBS technique for quantitative electron probe analysis using a lithium-drifted silicon detector. *Computers and Geosciences*, 7, 167–184.
- Zaitsev, A.I., Shelkova, N.E., Lyakishev, N.P., and Mogutnov, B.M. (1999) Thermodynamic properties and phase equilibria in the Na₂O-SiO₂ system. *Physical Chemistry Chemical Physics*, 1, 1899–1907.

MANUSCRIPT RECEIVED AUGUST 16, 2004

MANUSCRIPT ACCEPTED NOVEMBER 2, 2004

MANUSCRIPT HANDLED BY ROBERT F. DYMEK